International Journal of Modern Physics C, Vol. 8, No. 4 (1997) 859–867


# SYMMETRY BREAKING OF FLOW IN 2D SYMMETRIC CHANNELS: SIMULATIONS BY LATTICE-BOLTZMANN METHOD

LI-SHI LUO
*ICASE, Mail Stop 403, NASA Langley Research Center*
*6 North Dryden St., Bldg 1298*
*Hampton, Virginia 23681-0001, USA*
*and*
*Complex Systems Group (T-13), MS-B213, Theoretical (T) Division*
*Los Alamos National Laboratory*
*Los Alamos, New Mexico 87545, USA*
*E-mail*: *luo@icase.edu*

Received 4 November 1996
Revised 6 February 1997

In this paper, a numerical study of nonlinear flow phenomena in two-dimensional symmetric channels using the lattice-Boltzmann equation method is presented. The results are compared with both experimental results and other numerical results using some traditional methods. Comparisons are found to be quantitatively accurate.

*Keywords*: Lattice-Boltzmann and Lattice-BGK Methods; Symmetry Breaking; Flow in 2D Symmetric Channel with Expansion.

## 1. Introduction

The lattice-Boltzmann equation (LBE) is a new and intrinsically parallel algorithm utilizing massively parallel processors (MPP) to solve various partial differential equations.[1–5] The LBE method has demonstrated a broad scope of applicability to various fields such as hydrodynamics in porous media, multi-phase or multi-component flows, reactive chemical flow, magneto-hydrodynamics, etc. Because of the broad scope and great potential of its applications, the LBE method has been viewed not only as a novel technique, but also as a new and general approach in the spirit of kinetic theory for the study of complex systems.

Since LBE is a newly developed method and is still in its infancy, most numerical results obtained with this technique are qualitative in nature. (See, for example, results in the collective works edited by Doolen[4] and the recent reviews by Benzi *et al.*[5] and by Qian *et al.*[6]) High precision results of numerical simulations by the LBE method (e.g., work by Hou *et al.*[7]) are rarely available. Also, since the LBE method can handle complex boundary geometry easily, many LBE simulations have no counterpart produced with traditional numerical methods with which to

compare. Thus, there is a pressing need for high quality numerical benchmarks using the LBE method which can be compared with the results obtained by traditional methods or by experiments.

In this paper, a numerical study of nonlinear phenomena in a two-dimensional symmetric sudden-expansion channel flow using the LBE method is presented. The reason this system is chosen is that, not only does it exhibit an array of interesting nonlinear flow phenomena, but also it has been studied, to a great extent, both experimentally[8–12] and numerically[11,13,14] using some traditional methods, so that a comparative study between the LBE method and other traditional methods can be conducted quantitatively.

This paper is organized as follows. Section 2 provides a brief introduction of the LBE method. Section 3 describes the flow system of a 2D symmetric channel with expansion, and provides the details in the numerical simulation. Section 4 presents the numerical results of the simulations, and the comparison with experimental and other numerical results. Section 5 concludes the paper with discussions of the results and possible future work.

## 2. Lattice-Boltzmann Equation and Its Hydrodynamics

The first LBE model[1] is a straightforward floating-point-number counterpart of the Frisch, Hasslacher, and Pomeau (FHP) LGA model.[15,16] It is an evolution equation on a triangular lattice structure:

$$f_\alpha(\boldsymbol{x} + \hat{\boldsymbol{e}}_\alpha,\, t+1) = f_\alpha(\boldsymbol{x},\, t) + \Omega_\alpha\,, \tag{1}$$

where $\hat{\boldsymbol{e}}_\alpha = \cos[(\alpha-1)\pi/3]\hat{\boldsymbol{x}} + \sin[(\alpha-1)\pi/3]\hat{\boldsymbol{y}}$, $\alpha \in \{1,\, 2, \ldots,\, b\}$, are the velocity vectors along the links of the triangular lattice, $b$ is the number of the velocities $\hat{\boldsymbol{e}}_\alpha$ and is equal to 6 for FHP 6-bit or 7-bit models, and $\Omega$ is the collision operator. It can be shown that through the Chapman–Enskog procedure and with certain approximations, one can derive the Navier–Stokes equation from Eq. (1):[15–17]

$$\frac{\partial \boldsymbol{u}}{\partial t} + \boldsymbol{u}\cdot\nabla\boldsymbol{u} = -\frac{1}{\rho}\nabla P + \nu\nabla^2\boldsymbol{u}\,, \tag{2}$$

where $\nu$ is the kinetic viscosity depending on the eigenvalues of the collision operator $\Omega$.[17,18]

In Eq. (1), the collision operator is a $b \times b$ (or $(b+1)\times(b+1)$ depending on whether there are rest particles) matrix with the same rotational symmetry of the lattice structure.[17,18] With the single relaxation time approximation (or BGK approximation),[19,20] the collision operator can be characterized by a single parameter — the single relaxation time, $\tau$, and Eq. (1) can be simplified to

$$f_\alpha(\boldsymbol{x} + \hat{\boldsymbol{e}}_\alpha,\, t+1) = f_\alpha(\boldsymbol{x},\, t) - \frac{1}{\tau}[f_\alpha(\boldsymbol{x},\, t) - f_\alpha^{(\mathrm{eq})}(\boldsymbol{x},\, t)]\,. \tag{3}$$

With a properly chosen equilibrium distribution function, $f_\alpha^{(\mathrm{eq})}$, the Navier–Stokes equation (2) can be derived from Eq. (3) *via* the Chapman–Enskog procedure. The

following equilibrium distribution function can lead to the Navier–Stokes equation (2):

$$f_\alpha^{(\mathrm{eq})}(\boldsymbol{x},\, t) = \begin{cases} \rho(r - \boldsymbol{u}^2) & \alpha = 0\,, \\ \dfrac{1}{6}\rho((1-r) + 2(\hat{\boldsymbol{e}}_\alpha \cdot \boldsymbol{u}) + 4(\hat{\boldsymbol{e}}_\alpha \cdot \boldsymbol{u})^2 - \boldsymbol{u}^2) & \alpha \neq 0\,, \end{cases} \tag{4}$$

where $f_0^{(\mathrm{eq})}$ is the equilibrium distribution function for rest particles, $r$ is the fraction of rest particle density out of the total mass density. The ratio $r$ can be adjusted between 0 and 1 to change the sound speed. The distribution function of rest particles is included to give the correct ideal gas equation of state.[2,3,17] With the above equilibrium distribution function, the viscosity of the system is

$$\nu = \frac{1}{8}(2\tau - 1)\,, \tag{5}$$

and the sound speed is

$$c_s = \sqrt{\frac{(1-r)}{2}}\,. \tag{6}$$

## 3. Description of the System and Arrangement of the Simulation

In the past two decades, it has been of great interest to study certain flow systems experiencing transition to turbulence. One popular example is Taylor–Couette flow.[21,22] The flow in a symmetric sudden-expansion channel serves as another example. It has been observed experimentally that, below a certain critical value of the Reynolds number, depending on the geometric configuration of the channel, the flow pattern in a symmetric sudden-expansion channel is symmetric. The two recirculation regions behind the steps are symmetrically located with respect to the channel center plane. Also the flow is steady and two-dimensional at this stage. The symmetric flow becomes unstable once the Reynolds number exceeds the critical value, and a pair of steady asymmetric flows are observed as one recirculation region grows at the expense of the other — a symmetry-breaking bifurcation has taken place. The flow is still two-dimensional at this point. As the Reynolds number increases further, various instabilities may be observed, depending upon the geometric configuration of the channel. The flow may become first three-dimensional and then oscillatory or *vice versa*. Ultimately, the flow becomes turbulent as the Reynolds number increases further. Studies have shown that flow asymmetry and hence solution multiplicity remains a feature of flows in the turbulent regime.

Figure 1 shows a schematic two-dimensional plot (in $xy$-plane) of the flow channel in the experiment.[11] The main channel is an $1:3$ symmetric, plane expansion into a section of 80 step-heights in length and of aspect ratio $8:1$. Experimental observations have shown that the low Reynolds number flow ($R_e \leq 140$) is nominally two-dimensional in a channel with such an aspect ratio.[9,11]

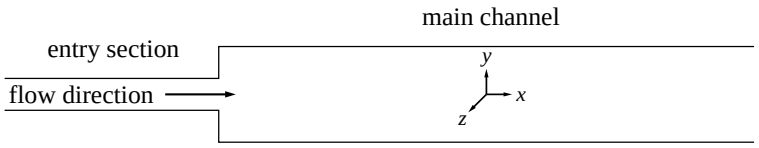


Fig. 1. A schematic two-dimensional plot of the flow channel in the experiment.

The Reynolds number for the system is defined as

$$R_e = \frac{hU_0}{2\nu}\,, \tag{7}$$

where $h$ is the height of the entry section, $U_0$ the maximum inlet velocity and $\nu$ the kinematic viscosity. The Reynolds number is tuned by changing $U_0$ in experiments with fixed $\nu$ and $h$.

To test the validity of the lattice-Boltzmann method, this algorithm is employed to study the occurrence of the symmetry-breaking bifurcation of the flow in the symmetric sudden-expansion channel. Because the bifurcation occurs at a critical Reynolds number at which the flow is two-dimensional, the two-dimensional lattice-BGK equation with triangular lattice spacing is used for the simulations. There are two boundary geometries used in the simulations, as shown in Fig. 2. At the entry, the flow velocity is prescribed in the following fashion. The $x$-component of velocity, $v_x$, has a parabolic profile with a maximum, $U_0$, while the $y$-component, $v_y$, is zero. This entry profile is fixed for all time. At the boundary walls, velocity is always set to be zero. In the algorithm used here, the number of rest particles equals the number of moving particles, that is $r = 1/2$. Thus the sound speed, $c_s$, is $1/2$ according to Eq. (6), and the Reynolds number is

$$R_e = \frac{4hU_0}{2\tau - 1}\,, \tag{8}$$

where $h = \frac{\sqrt{(8)}}{2}N_0$, and $N_0$ is the number of lattice sites in the $\boldsymbol{y}$-direction at the entry. The Reynolds number is varied by changing $\tau$, with both $h$ and $U_0$ fixed.

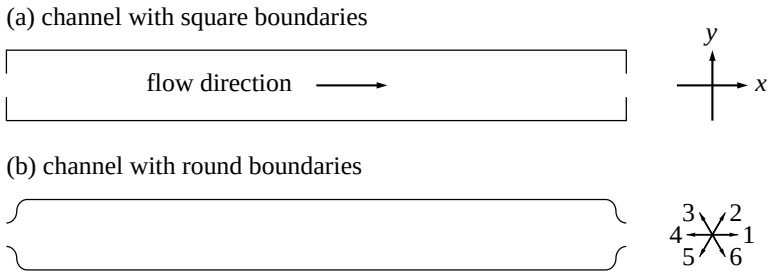


Fig. 2. Geometry of boundary walls used in the simulations.

## 4. Numerical Results for the Steady State Symmetry-Breaking Bifurcation

In what follows, only the results of simulations with a system size of $N_x \times N_y = 2048 \times 256$ are reported. (Smaller system sizes, $512 \times 64$ and $1024 \times 128$, are also used in simulations to test convergence.) The height of the entry section is 86 lattice sites (in $\boldsymbol{y}$-direction), thus $h = 43\sqrt{3}$. The maximum speed at entry $U_0 = 0.15$. The sinusoidal boundary walls are prescribed by $y = \pm f(x)$, where

$$f(x) = \begin{cases} \dfrac{h}{2} + \dfrac{(L_y - h)}{2}(1 - \cos((x-1)\pi/64))\,, & 1 \le x \le 64\,, \\ \dfrac{L_y}{2}\,, & 65 \le x \le L_x - 64\,, \\ \dfrac{h}{2} + \dfrac{(L_y - h)}{2}(1 - \cos((L_x - x)\pi/64))\,, & L_x - 63 \le x \le L_x\,. \end{cases}$$

Note that the values of $y$ are integers. With the configuration of the channel shown in Fig. 2, the expansion ratio is $\frac{86}{256} \approx \frac{1}{3}$. With the given $h$ and $U_0$, the Reynolds number is

$$R_e = \frac{25.8\sqrt{3}}{2\tau - 1}\,.$$

The boundary conditions of the simulation are set as follows. At the entrance, $v_y = 0$, and a parabolic velocity profile with maximum $U_0 = 0.15$ for $v_x$ is enforced. At the exit, the fully-developed or stress boundary condition, $\partial \boldsymbol{v}/\partial x = 0$, is applied. At the walls, the simple bounce-back boundary condition is used. The initial conditions for the velocity field in our simulations are set to be asymmetric with respect to the symmetric $x$-axis of the channel, $v_x(y > 0) = 0.01$, $v_x(y < 0) = 0$, and $v_y = 0$. The asymmetry of the initial condition determines the branch the asymmetric final state reaches. The simulation is run until a steady state is achieved.

We define the stream function,

$$\psi(x,\, y) = \int_0^y v_x(x,\, y')dy'\,, \tag{9}$$

and a variable of state, $\chi$, to measure the asymmetry:

$$\chi^2 = \frac{\displaystyle\int [\psi(x,\, y) + \psi(x,\, -y)]^2 dxdy}{\displaystyle\int dxdy} \approx \frac{\displaystyle\sum_{i,\,j=1}^{N_x,\,N_y} [\psi(x_i,\, y_j) + \psi(x_i,\, -y_j)]^2}{N_x \times N_y}\,. \tag{10}$$

It is obvious that when the flow pattern is symmetric about the $x$-axis, $\chi = 0$. In the simulations, $\chi$ is measured as a function of $R_e$.

Figures 3 and 4 are contours of the steady-state stream function for different values of $R_e$. The symmetric flow pattern for $R_e$ below the symmetry-breaking

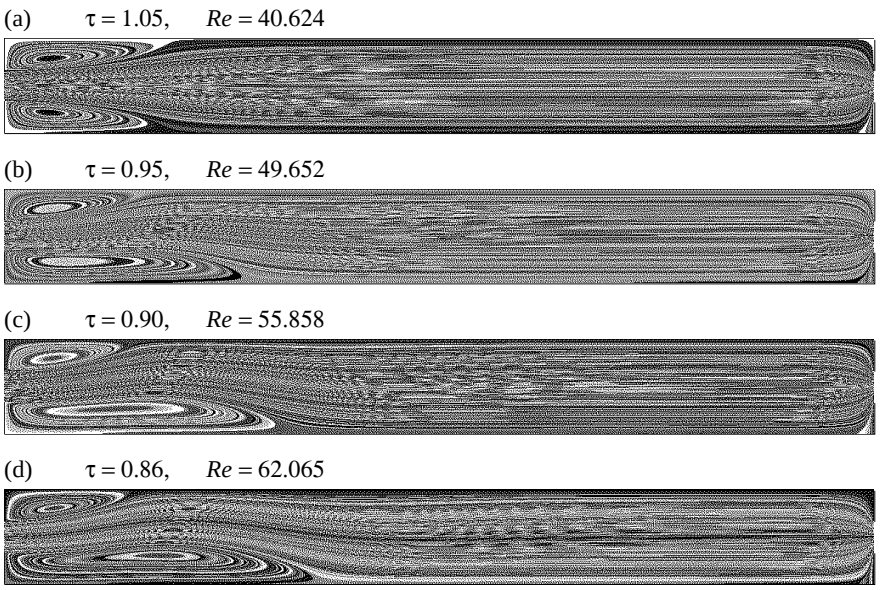


Fig. 3. The contours of the stream function for the channel flow with square wall. (a), with $R_e = 40.624$, illustrates the symmetric flow pattern before the symmetry-breaking bifurcation occurs. (b) $R_e = 49.652$, (c) $R_e = 55.858$, and (d) $R_e = 62.065$, illustrate the asymmetric flow patterns developed after the symmetry-breaking bifurcation occurs.

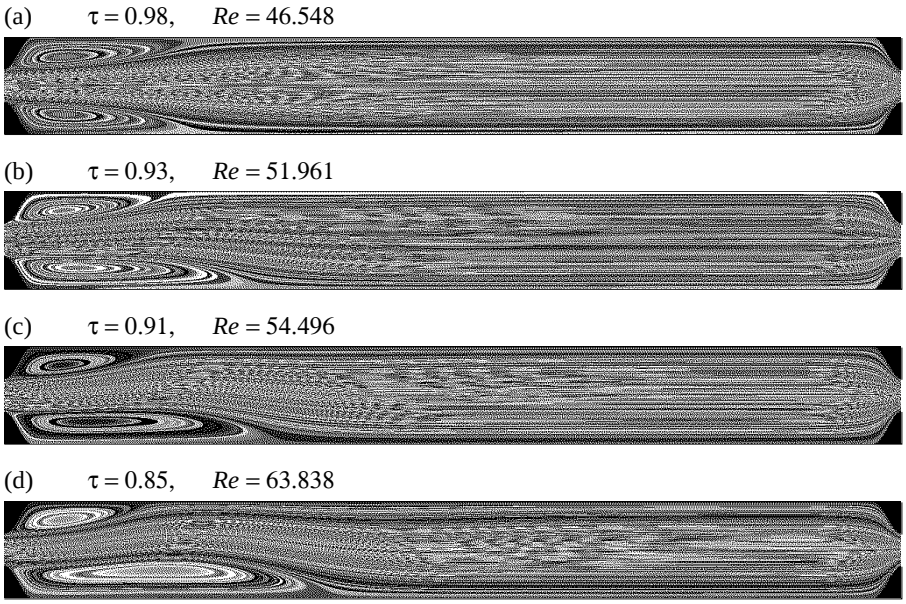


Fig. 4. The same as Fig. 3, with the sinusoidal walls. (a) $R_e = 46.548$, (b) $R_e = 51.961$, (c) $R_e = 54.496$, and (d) $R_e = 63.838$.

bifurcation and the asymmetric ones for $R_e$ above the bifurcation are shown clearly in Figs. 3 and 4.

Figure 5 is the bifurcation diagram for the symmetry-breaking bifurcation in the channel flow. The diagram clearly shows the existence of the symmetry-breaking bifurcation at the critical Reynolds number, $R_e^*$. For the channel with square boundaries, we found that $R_e^* = 46.19$. For the channel with the sinusoidal boundaries, $R_e^* = 50.12$. To test the stability of the solutions, random noise with magnitude of 10% $U_0$ is added to $v_x$ and $v_y$ at the entry. The results indicate that solutions are stable under the disturbance.

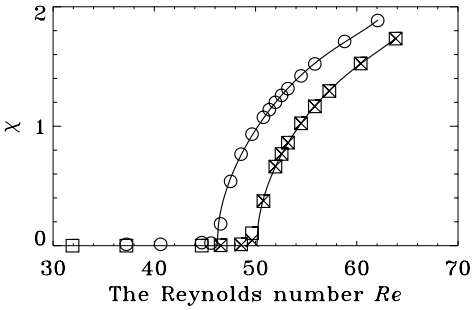


Fig. 5. Bifurcation diagram of the symmetry-breaking bifurcation for low in the symmetric sudden-expansion channel. Symbol × represents the values of $\chi$ with the sinusoidal walls; □ represents $\chi$ with the sinusoidal walls and with random force at the entry; ◯ represents $\chi$ with the square walls.

We have also used $\chi$ as a measure of convergence in our simulations. At the Reynolds number lower than $R_e^*$, $\chi$ goes to zero with an asymmetric initial condition as the number of iterations $t \to \infty$. However, the value of $\chi$, with which the system reaches its steady state, is not exactly zero and it depends on the system size in the simulation. We observed that with $R_e \approx 5$ fixed, the values of $\chi$ at the steady state of the system decays to zero as $N^{-2}$, where $N$ is the number of lattice sites along any one dimension of the system. The observation was made with three different system sizes, $N_x \times N_y = 512 \times 64$, $1024 \times 128$, and $2048 \times 256$.

## 5. Discussion and Conclusion

In the work by Fearn *et al.*,[11] a channel with square boundaries was used in both numerical simulations and laboratory experiments. The values of the critical Reynolds number obtained from their numerical simulations and their experiments were $R_e^* = 40.45$ and 47.3, respectively. Our numerical results ($R_e^* = 46.19$) not only reconfirm the existence of the symmetry-breaking bifurcation for flow in the 2D symmetric sudden-expansion channel, but also agree with the existing results in the work by Fearn *et al.*[11] quantitatively. In the numerical work by Sobey and Drazin,[13] the value of $R_e^* = 5.95$ was obtained for the channel with the sinusoidal walls. Considering the difference in the definition of the Reynolds number, $R_e$, the

quantitative disagreement still cannot be resolved between the results in these two references.[11,13] However, it is clearly understood that the value of $R_e^*$ for the channel with sudden expansion must be less than that for the channel with sinusoidal expansion. Therefore, it can be concluded that the numerical value of $R_e^*$ obtained by Sobey and Drazin[13] is erroneous.

As shown in the results, the value of $R_e^*$ sensitively depends upon the boundary geometry. The values of $R_e^*$ for two sets of boundaries, i.e., the square and the sinusoidal walls illustrated in Fig. 2, are different. The bifurcation in the symmetric channel is not generic in the sense that the bifurcation exists because of the symmetry of the boundary geometry. Therefore, it is plausible that one expects the stability of the symmetric mode (or the asymmetric modes) in the problem to depend upon the boundary conditions. This boundary condition sensitivity could also contribute, at least in part, to the difference between the results here and those obtained by the standard methods. (Indeed, Fearn *et al.*[11] also attribute the difference between the experimental results and the numerical ones to the sensitive dependence of the system on the boundary conditions.) Although, in the limit of an infinitely large lattice system, the lattice-gas or the lattice-Boltzmann algorithms should converge to the Navier–Stokes equation. But, with the finite-size system, differences between kinetic models and PDEs are visible. (Note that the difference between our result here and the result of Fearn *et al.*[11] is greater than 10% in terms of $R_e^*$.)

In conclusion, we have demonstrated that the LBE method can be used to simulate hydrodynamic systems. Our results presented in this paper are quantitatively accurate when compared with the existing experimental and numerical results. The advantages of the LBE method are that it is simple to program and fast to process on parallel computers. We hope to use the LBE algorithm to study the flow in a symmetric expansion channel with a higher Reynolds number and in three-dimensional space in the near future.

## Acknowledgments

The author would like to express his gratitude to Dr. Gary Doolen and Dr. Shiyi Chen for their support and encouragement during this work. The author would also like to thank Dr. Hudong Chen, Dr. Xiaoyi He, Prof. D. d'Humières, and Dr. Basil Nichols for helpful discussions. The editorial assistance of Mr. David V. Brydon is gratefully acknowledged. This work first appeared in the author's Ph.D. thesis.[17]

## References

1. G. McNamara and G. Zanetti, *Phys. Rev. Lett.* **61**, 2332 (1988).
2. H. Chen, S. Chen, and W. H. Matthaeus, *Phys. Rev.* **A45**, R5339 (1991).
3. Y. H. Qian, D. d'Humières, and P. Lallemand, *Europhys. Lett.* **17**, 479 (1992).
4. Gary D. Doolen (ed.), *Lattice Gas Methods for Partial Differential Equations* (Addison-Wesley, Redwood City, California, 1990).
5. R. Benzi, S. Succi, and M. Vergassola, *Phys. Rep.* **222**, 145 (1992).

6. Y.-H. Qian, S. Succi, and S. A. Orszag, in *Annual Review of Computational Physics*, Vol. **III**, D. Stauffer (ed.), (Word Scientific, Singapore, 1995).
7. S. Hou, Q. Zou, S. Chen, G. Doolen, and A. C. Cogley, *J. Comp. Phys.* **118**, 329 (1995).
8. F. Durst, A. Melling, and J. H. Whitelaw, *J. Fluid Mech.* **64**, 111 (1974).
9. W. Cherdron, F. Durst, and J. H. Whitelaw, *J. Fluid Mech.* **84**, 13 (1978).
10. I. Sobey, *J. Fluid Mech.* **151**, 395 (1985).
11. R. M. Fearn, T. Mullin, and K. A. Cliffe, *J. Fluid Mech.* **211**, 595 (1990).
12. F. Durst, J. C. F. Pereira, and C. Tropea, *J. Fluid Mech.* **248**, 567 (1993).
13. I. Sobey and P. G. Drazin, *J. Fluid Mech.* **171**, 263 (1986).
14. L. Kaiktsis, "Break of Symmetry and Early Transition in a Symmetric Sudden Expansion Flow," preprint, May 1992.
15. U. Frisch, B. Hasslacher, and Y. Pomeau, *Phys. Rev. Lett.* **56**, 1505 (1986).
16. S. Wolfram, *J. Stat. Phys.* **45**, 471 (1985).
17. L.-S. Luo, *Lattice-gas automata and lattice-Boltzmann equations for two-dimensional hydrodynamics*, Ph.D. thesis, Georgia Institute of Technology, Atlanta, 1993.
18. L.-S. Luo, H. Chen, S. Chen, G. D. Doolen, and Y.-C. Lee, *Phys. Rev.* **A43**, R7097 (1991).
19. P. L. Bhatnagar, E. P. Gross, and M. Krook, *Phys. Rev.* **94**, 511 (1954).
20. R. L. Liboff, *Kinetic Theory* (Prentice Hall, Englewood Cliff, New Jersey, 1990).
21. R. C. DiPrima and H. L. Swinney, in *Hydrodynamics Instabilities and the Transition to Turbulence*, 2nd edition, H. L. Swinney and J. P. Gullob (eds.), (Springer-Verlag, Berlin, 1985), Chapter 6.
22. T. Mullin and K. A. Cliffe, in *Nonlinear Phenomena and Chaos*, S. Sarker (ed.), (Adam Hilger, Bristol, 1986).